

Basic Study

Propofol induces ferroptosis and inhibits malignant phenotypes of gastric cancer cells by regulating miR-125b-5p/STAT3 axis

Yi-Ping Liu, Zhong-Zhi Qiu, Xu-Hui Li, En-You Li

ORCID number: Yi-Ping Liu 0000-0001-9992-8789; Zhong-Zhi Qiu 0000-0001-5463-7646; Xu-Hui Li 0000-0002-7887-4440; En-You Li 0000-0001-9594-2508.

Author contributions: Liu YP and Qiu ZZ designed the study; Liu YP and Li XH performed the experiments; Qiu ZZ collected and analyzed data; Li EY wrote the manuscript.

Institutional review board

statement: This study was reviewed and approved by the Ethics Committee of the First Affiliated Hospital of Harbin Medical University.

Institutional animal care and use

committee statement: All animal experiments were performed under the approval of Animal Ethics Committee of The First Affiliated Hospital of Harbin Medical University.

Conflict-of-interest statement: The authors declare no conflict of interest.

Data sharing statement: No additional data are available.

ARRIVE guidelines statement: The authors have read the ARRIVE Guidelines, and the manuscript was prepared and revised

Yi-Ping Liu, Zhong-Zhi Qiu, En-You Li, Department of Anesthesiology, First Affiliated Hospital of Harbin Medical University, Harbin 150001, Heilongjiang Province, China

Xu-Hui Li, Department of Gastroenterology, Heilongjiang Forest Industry Federation (Red Cross) Hospital, Harbin 150008, Heilongjiang Province, China

Corresponding author: En-You Li, PhD, Chief Physician, Department of Anesthesiology, First Affiliated Hospital of Harbin Medical University, No. 23 Youzheng Street, Nangang District, Harbin 150001, Heilongjiang Province, China. enyouli@sina.com

Abstract

BACKGROUND

Gastric cancer is a common malignancy with poor prognosis, in which ferroptosis plays a crucial function in its development. Propofol is a widely used anesthetic and has antitumor potential in gastric cancer. However, the effect of propofol on ferroptosis during gastric cancer progression remains unreported.

AIM

To explore the function of propofol in the regulation of ferroptosis and malignant phenotypes of gastric cancer cells.

METHODS

MTT assays, colony formation assays, Transwell assays, wound healing assay, analysis of apoptosis, ferroptosis measurement, luciferase reporter gene assay, and quantitative reverse transcription polymerase chain reaction were used in this study.

RESULTS

Our data showed that propofol was able to inhibit proliferation and induce apoptosis of gastric cancer cells. Meanwhile, propofol markedly repressed the invasion and migration of gastric cancer cells. Importantly, propofol enhanced the erastin-induced inhibition of growth of gastric cancer cells. Consistently, propofol increased the levels of reactive oxygen species, iron, and Fe²⁺ in gastric cancer cells. Moreover, propofol suppressed signal transducer and activator of transcription (STAT)3 expression by upregulating miR-125b-5p and propofol induced ferroptosis by targeting STAT3 in gastric cancer cells. The miR-125b-5p inhibitor or STAT3 overexpression reversed propofol-attenuated malignant phenotypes of gastric cancer cells.

according to the ARRIVE Guidelines.

Country/Territory of origin: China

Specialty type: Gastroenterology and hepatology

Provenance and peer review: Unsolicited article; Externally peer reviewed.

Peer-review report's scientific quality classification

Grade A (Excellent): 0
Grade B (Very good): B
Grade C (Good): C
Grade D (Fair): 0
Grade E (Poor): 0

Open-Access: This article is an open-access article that was selected by an in-house editor and fully peer-reviewed by external reviewers. It is distributed in accordance with the Creative Commons Attribution NonCommercial (CC BY-NC 4.0) license, which permits others to distribute, remix, adapt, build upon this work non-commercially, and license their derivative works on different terms, provided the original work is properly cited and the use is non-commercial. See: <http://creativecommons.org/licenses/by-nc/4.0/>

Received: July 6, 2021

Peer-review started: July 6, 2021

First decision: July 26, 2021

Revised: September 10, 2021

Accepted: October 25, 2021

Article in press: October 25, 2021

Published online: December 15, 2021

P-Reviewer: Chisthi MM, Yashiro M

S-Editor: Gong ZM

L-Editor: Kerr C

P-Editor: Gong ZM



CONCLUSION

Propofol induced ferroptosis and inhibited malignant phenotypes of gastric cancer cells by regulating the miR-125b-5p/STAT3 axis. Propofol may serve as a potential therapeutic candidate for gastric cancer.

Key Words: Gastric cancer; Progression; Ferroptosis; Propofol; miR-125b-5p; STAT3

©The Author(s) 2021. Published by Baishideng Publishing Group Inc. All rights reserved.

Core Tip: In this study, we discovered that propofol induced ferroptosis and inhibited malignant phenotypes of gastric cancer cells by regulating the miR-125b-5p/STAT3 axis. Propofol may serve as a potential therapeutic candidate for gastric cancer.

Citation: Liu YP, Qiu ZZ, Li XH, Li EY. Propofol induces ferroptosis and inhibits malignant phenotypes of gastric cancer cells by regulating miR-125b-5p/STAT3 axis. *World J Gastrointest Oncol* 2021; 13(12): 2114-2128

URL: <https://www.wjgnet.com/1948-5204/full/v13/i12/2114.htm>

DOI: <https://dx.doi.org/10.4251/wjgo.v13.i12.2114>

INTRODUCTION

Gastric cancer is a severe, lethal type of cancer worldwide[1]. Despite improvement in treatment, gastric cancer remains the leading cause of cancer-associated death[2]. Adjuvant therapy, radical surgery, and early diagnosis enhance survival rates and prognosis for gastric cancer, but mortality is still unsatisfactory[3,4]. Ferroptosis is a type of regulated cell death that differs from apoptosis and is repressed by erastin, especially in RAS-mutated cancer cells[5]. It has been identified that the suppression of ferroptosis contributes to cancer progression, and ferroptosis has a crucial role in the development of gastric cancer[6-8]. However, the exploration of a treatment that can target ferroptosis is still limited.

Propofol is a broadly applied anesthetic because of rapid recovery and has some nonanesthetic functions in cancer development[9]. It has been identified that propofol inhibits cell invasion and growth and induces apoptosis in pancreatic cancer[10]. Meanwhile, propofol decreases cell proliferation and increases apoptosis of lung cancer cells by regulating caspases-3, Bim, forkhead box (FOX)O1, and FOXO3, in which miR-486 inhibitor can reverse this effect[11]. Propofol also represses the malignant progression of promyelocytic leukemia cells[12]. Moreover, it has been reported that propofol induces an inhibitory effect on gastric cancer cell invasion and migration in patients with gastric cancer[13,14]. However, the function of propofol in the modulation of ferroptosis during gastric cancer progression remains elusive. miRNAs can modulate gene expression in different cellular processes[15]. Previous studies have revealed that miRNAs participate in the development of gastric cancer [16,17]. Meanwhile, a recent study has shown that miR-125b-5p is a tumor suppressor and involved in the modulation of gastric cancer[18]. In addition, signal transducer and activator of transcription (STAT)3 has been identified as an oncogene in gastric cancer[19-21]. However, the effect of propofol on miR-125b-5p and STAT3 during the development of gastric cancer remains obscure.

In this study, we focused on the investigation of the function of propofol in the development of gastric cancer. We found that propofol induced ferroptosis and inhibited malignant phenotypes of gastric cancer cells by regulating the miR-125b-5p/STAT3 axis.

MATERIALS AND METHODS

Cell culture

The SGC7901 and BGC823 cells were maintained in the laboratory. The cells were cultured in Dulbecco's modified Eagle's medium (DMEM; Solarbio, China) with 0.1 mg/mL streptomycin (Solarbio), 100 U/mL penicillin (Solarbio), and 10% fetal bovine

serum (Solarbio), under the conditions of 37 °C with 5% CO₂. The pcDNA3.1-STAT3 overexpression vector, miR-125b-5p mimic, miR-125b-5p inhibitor, and corresponding control were purchased from Genscript Biotech Corporation (Nanjing, China) and GenePharma Co. Ltd. (Shanghai, China). The transfection in the cells was performed by Liposome 3000 (Invitrogen, Carlsbad, CA, United States). Propofol was purchased from Sigma (St. Louis, MO, United States).

MTT assays

SGC7901 and BGC823 cells were treated with propofol for 48 h. MTT assays analyzed the proliferation of SGC7901 and BGC823 cells. About 2×10^5 cells were plated in 96-well plates and incubated for 24 h. To assess cell viability, the cells were cultured with MTT solution (5 mg/mL) and incubated for 4 h, and 150 μ L dimethyl sulfoxide (DMSO) was applied to treat the cells. The cell viability was measured at 570 nm absorbance by applying an ELISA browser (Bio-Tek EL 800, Winooski, VT, United States).

Colony formation assays

The SGC7901 and BGC823 cells were treated with propofol for 48 h. Colony formation assays measured proliferation. About 10^4 SGC7901 and BGC823 cells were placed in six-well plates and cultured in DMEM at 37 °C. The cells were cleaned with phosphate-buffered saline (PBS) after 2 wk, washed in methanol for ~30 min, and stained with 1% crystal violet dye, after which, the number of colonies was calculated.

Transwell assays

To analyze cell migration, the cells were cultured for 24 h and resuspended in serum-free culture medium, then plated into the apical chamber of a Transwell chamber at 5×10^3 cells/well. The culture medium was made up to 150 μ L and 600 μ L complete culture medium was added to the basolateral chamber. After 24 h culture at 37°C and 5% CO₂, the cells were fixed with 4% paraformaldehyde for 10 min, stained by crystal violet dye for 20 min, followed by analysis using the intelligent biological navigator (Olympus, Tokyo, Japan). The migrated cells were recorded and calculated by using the ImageJ software.

To analyze cell invasion, Matrigel was melted overnight at 4 °C and diluted by presold serum-free culture medium (ratio 8:1). The medium (50 μ L) was plated into the Transwell polycarbonate membrane with a pore diameter of 8 μ m, covering all the wells with Matrigel at 37°C for 2 h. The cells were cultured for 24 h and resuspended in serum-free culture medium, plated into the Transwell apical chamber at 10^5 cells/well, and the medium was made up to 150 μ L. Complete medium with 50% FBS (600 μ L) was added to the basolateral chamber. After 24 h, the cells were fixed using 4% paraformaldehyde for 15 min and stained with crystal violet dye for 10 min. The invaded cells were analyzed and calculated using the ImageJ software.

Wound healing assay

SGC7901 and BGC823 cells were treated with propofol for 48 h. Approximately 3×10^5 SGC7901 and BGC823 cells were plated into the 24-well plates and incubated overnight to reach a fully confluent monolayer. A 20- μ L pipette tip was applied to slowly cut a straight line across the well. The well was washed by PBS three times and the medium was changed to serum-free medium and culture was continued. The wound healing percentage was calculated.

Analysis of apoptosis

The SGC7901 and BGC823 cells were treated with propofol for 48 h. Approximately 2×10^5 SGC7901 and BGC823 cells were plated in six-well dishes. Apoptosis was determined using the Annexin V-FITC Apoptosis Detection Kit (Cell Signaling Technology, Danvers, MA, United States). About 2×10^5 washed cells were collected by binding buffer and stained at 25 °C, followed by flow cytometry analysis.

Ferroptosis measurement

SGC7901 and BGC823 cells were cotreated with erastin (5 mmol/L) or ferrostatin (1 mmol/L). After 48 h, the cell viability was analyzed by MTT assay. Elevated iron level and accumulated lipid reactive oxygen species (ROS) were representative characteristics of ferroptosis. We used an iron assay kit (Beyotime, China) to examine the level of intracellular Fe²⁺. The cells were homogenized to collect the supernatant, incubated with iron reducer, followed by labeling with iron probe. OD 590 nm was detected in a microplate reader (PerkinElmer, Waltham, MA, United States). For detection of lipid

ROS, cells were stained with BODIPY C-11 dye (Beyotime) for 30 min, and subsequently detected by flow cytometry (BD Biosciences, Franklin Lakes, NJ, United States). The levels of malondialdehyde (MDA) and glutathione peroxidase (GSH) was measured by the MDA detection kit (Beyotime) and GSH assay kit (Cayman, Ann Arbor, MI, United States), respectively.

Luciferase reporter gene assay

The luciferase reporter gene assays were performed using the Dual-luciferase Reporter Assay System (Promega, Madison, WI, United States). SGC7901 and BGC823 cells were treated with miR-125b-5p mimic, pmirGLO-STAT3 (contained STAT3 3'UTR), and pmirGLO-STAT3 mutant transfected into the cells using Lipofectamine 3000 (Invitrogen), followed by analysis of luciferase activities, in which Renilla was applied as a normalized control.

Quantitative reverse transcription polymerase chain reaction

Total RNA was extracted by TRIZOL (Invitrogen). The first-strand cDNA was manufactured according to the manufacturer's instructions (Thermo Fisher Scientific, Waltham, MA, United States). qRT-PCR was carried out by SYBR Real-time PCR I kit (Takara, Japan). The standard control for miRNA and mRNA/circRNA was U6 and GAPDH, respectively. Quantitative determination of the RNA levels was conducted in triplicate independent experiments. The primer sequences were as follows: miR-125b-5p forward: 5'-TCCCTGAGACCCTAACTTGTGA-3'; reverse: 5'-AGTCTCAGGGTC CGAGGTATTC-3'; STAT3 forward: 5'-GGCCATCTGAGCACTAAGC-3', reverse: 5'-CGGACTGGATCTGGGTCTTA-3'; GAPDH forward: 5'-TATGATGATATCAAGA GGGTAGT-3', reverse: 5'-TATGATGATATCAAGAGGGTAGT-3'; U6 forward: 5'-CTCGCTTCGGCAGCACA-3', U6 reverse: 5'-AACGCTTCACGAATT TGCCT-3'.

Western blot analysis

Total proteins were isolated from the cells with RIPA buffer (Cell Signaling Technology) and analyzed by BCA Protein Quantification Kit (Abbkine, United States). The protein was separated by 12% SDS-PAGE, and transferred to polyvinylidene difluoride membranes (Millipore, Billerica, MA, United States). The membranes were treated with 5% milk and incubated overnight at 4°C with the primary antibodies for STAT3 (Rabbit monoclonal, 1:1000, diluted by 5% milk; Cell Signaling Technology), GPX4 (Rabbit monoclonal, 1:1000, diluted by 5% milk; Cell Signaling Technology) and SLC7A11 (Rabbit monoclonal, 1:1000, diluted by 5% milk; Cell Signaling Technology); and β -actin (Mouse monoclonal, 1:1000, diluted by 5% milk; Cell Signaling Technology), E-cadherin (Rabbit monoclonal, 1:1000, diluted by 5% milk; Cell Signaling Technology) and vimentin (Rabbit monoclonal, 1:1000, diluted by 5% milk; Cell Signaling Technology), in which β -actin served as the control. The corresponding secondary antibodies (Abcam, Cambridge, MA, United States) were incubated with the membranes for 1 h at room temperature, followed by visualization using an Odyssey CLx Infrared Imaging System.

Xenograft assays

All animal experiments were performed under the approval of Animal Ethics Committee of The First Affiliated Hospital of Harbin Medical University. Specific-pathogen-free male nude mice aged 5-6 wk and weighted around 20 g were purchased from Vitalriver (China). All mice were maintained in a 12-h circadian rhythm, and had free access to water and food. SGC7901 and BGC823 cells were subcutaneously injected into the right flank of mice. Propofol (50 mg/kg/d) was administrated intraperitoneally after tumor volume approached 100 mm³ for 20 d[22]. For the control group, the mice were treated with an equal volume of DMSO. Tumor volume and body weight were monitored every 5 d. The tumor size was calculated using the formula: length \times width²/2.

Statistical analysis

Data were expressed as mean \pm SD, and the statistical analysis was conducted using GraphPad Prism 7. The unpaired Student's *t* test was used to compare two groups, and one-way analysis of variance was used to compare among multiple groups. *P* < 0.05 was considered statistically significant.

RESULTS

Propofol decreases proliferation and induces apoptosis of gastric cancer cells

We evaluated the effect of propofol on proliferation and apoptosis of gastric cancer cells. Propofol repressed viability of SGC7901 and BGC823 cells in a dose-dependent manner and 10 $\mu\text{mol/L}$ propofol had a greater effect, which was selected in the subsequent analysis (Supplementary Figure 1). Propofol was able to inhibit viability of SGC7901 and BGC823 cells (Figure 1A and B). Similarly, propofol markedly reduced proliferation of SGC7901 and BGC823 cells (Figure 1C and D). Apoptosis of SGC7901 and BGC823 cells was enhanced by propofol (Figure 1E and F), suggesting that propofol decreases proliferation and induces apoptosis of gastric cancer cells.

Propofol reduces invasion and migration of gastric cancer cells

We further measured the effect of propofol on the migration and invasion of gastric cancer cells. Transwell assays indicated that the migration and invasion of SGC7901 and BGC823 cells were markedly decreased by propofol (Figure 2A and B). Consistently, the treatment of propofol significantly repressed wound healing in SGC7901 and BGC823 cells (Figure 2C and D), indicating that propofol is able to attenuate the migration and invasion of gastric cancer cells. Consistently, propofol enhanced E-cadherin expression and reduced vimentin expression in SGC7901 and BGC823 cells (Figure 2E).

Propofol enhances ferroptosis in gastric cancer cells

To analyze the impact of propofol on ferroptosis, we assessed the role of propofol in the erastin-induced inhibition of cell growth and the intracellular levels of ROS, iron and Fe^{2+} , and expression of GPX4 and SLC7A11, which are considered to be ferroptosis markers. Propofol enhanced the erastin-induced inhibitory effect on SGC7901 and BGC823 cell growth, in which erastin served as an activator of ferroptosis (Figure 3A and B). Iron levels were induced by propofol in SGC7901 and BGC823 cells (Figure 3C). Propofol significantly promoted the levels of ROS in SGC7901 and BGC823 cells (Figure 3D). Propofol increased accumulation of Fe^{2+} in SGC7901 and BGC823 cells (Figure 3E). Consistently, the expression of GPX4 and SLC7A11 was inhibited by propofol in SGC7901 and BGC823 cells (Figure 3F). GSH levels were reduced and MDA levels were enhanced in SGC7901 and BGC823 cells by treatment with propofol (Figure 3G and H), suggesting that propofol enhances ferroptosis in gastric cancer cells.

Propofol represses STAT3 expression by upregulating miR-125b-5p in gastric cancer cells

We explored the potential mechanisms underlying propofol-mediated gastric cancer progression. Given that propofol can regulate colon cancer metastasis by regulating STAT3 signaling[23], we assessed the correlation of propofol with STAT3 in gastric cancer. Significantly, we identified that propofol was able to upregulate expression of miR-125b-5p in SGC7901 and BGC823 cells (Figure 4A). We identified the binding site between miR-125b-5p and STAT3 mRNA 3' UTR in a bioinformatic analysis using Targetscan (http://www.targetscan.org/vert_72/) (Figure 4B). Treatment with miR-125b-5p mimic reduced luciferase activities of wild-type STAT3, but not STAT3 with miR-125b-5p-binding site mutant in SGC7901 and BGC823 cells (Figure 4C and D). mRNA and protein expression of STAT3 was significantly suppressed by miR-125b-5p mimic in SGC7901 and BGC823 cells (Figure 4E). Propofol inhibited expression of STAT3, which was reversed by miR-125b-5p inhibitor (Figure 4F), indicating that propofol represses STAT3 expression by upregulating miR-125b-5p in gastric cancer cells.

Propofol enhances ferroptosis by targeting STAT3 in gastric cancer cells

We confirmed whether propofol modulated ferroptosis by targeting STAT3 in gastric cancer cells. As expected, overexpression of STAT3 was able to rescue propofol-inhibited cell growth in the erastin-treated SGC7901 and BGC823 cells (Figure 5A). Similarly, STAT3 overexpression reversed propofol-induced levels of Fe^{2+} , iron and ROS (Figure 5B-D), suggesting that propofol induces ferroptosis by inhibiting STAT3 in gastric cancer cells.

Propofol attenuates gastric cancer progression by miR-125b-5p/STAT3 axis

We further investigated the role of the propofol/miR-125b-5p/STAT3 axis in regulating gastric cancer malignant phenotypes. Overexpression of STAT3 or miR-

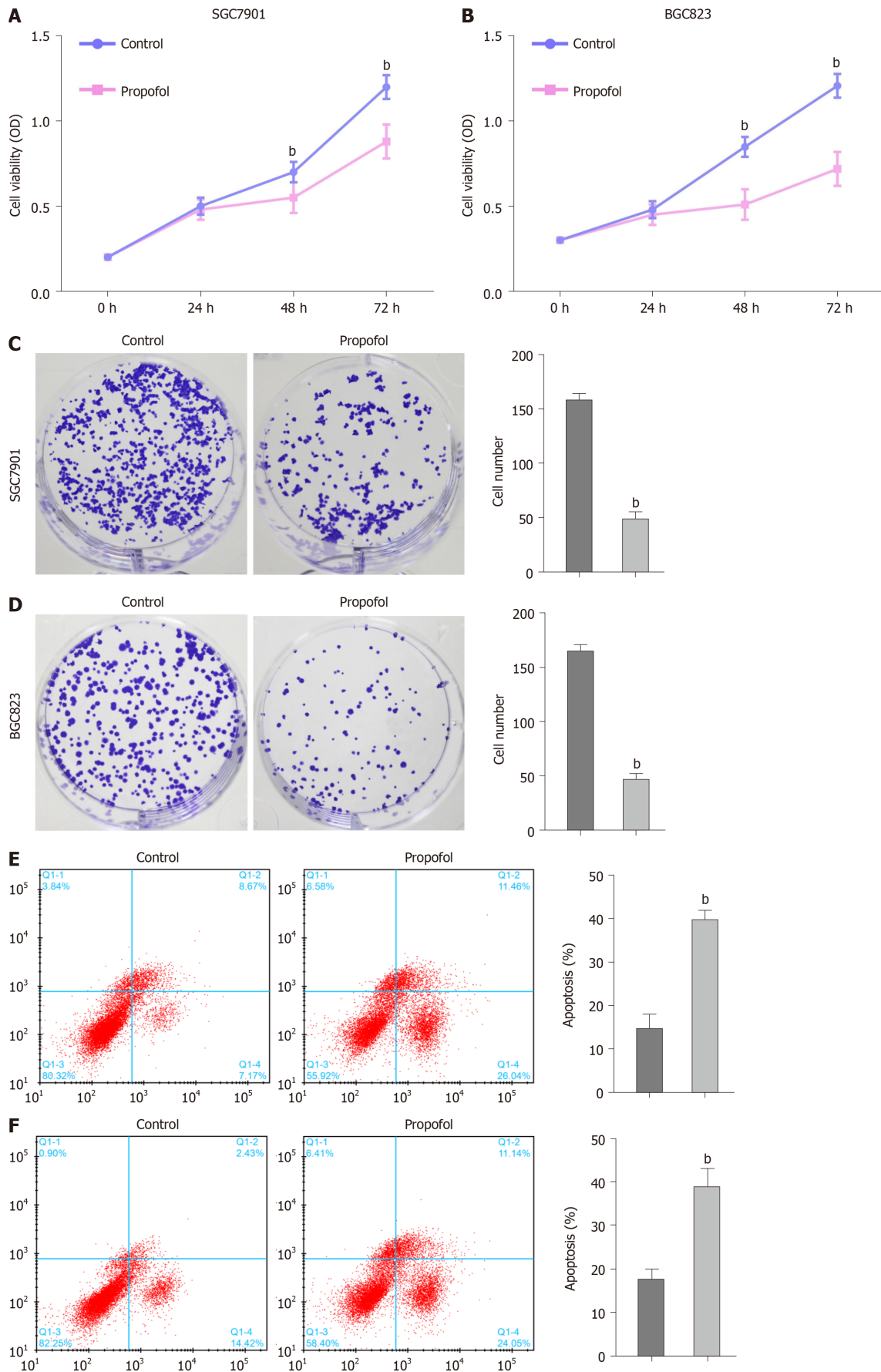
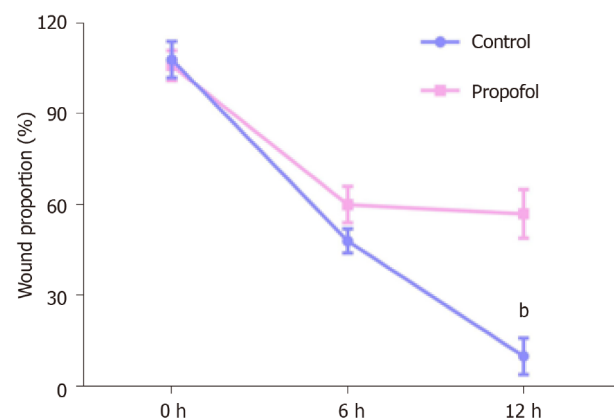
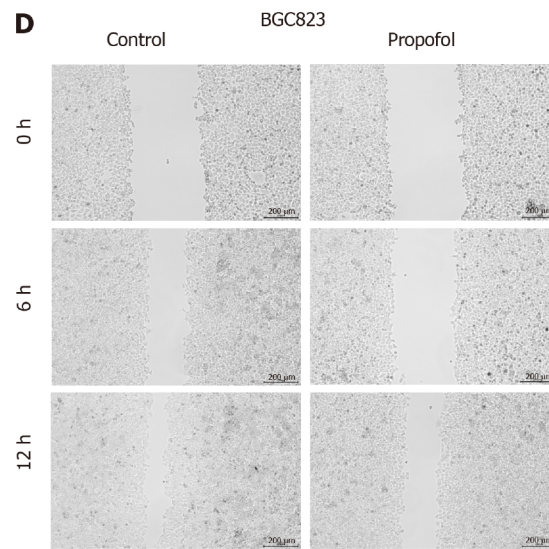
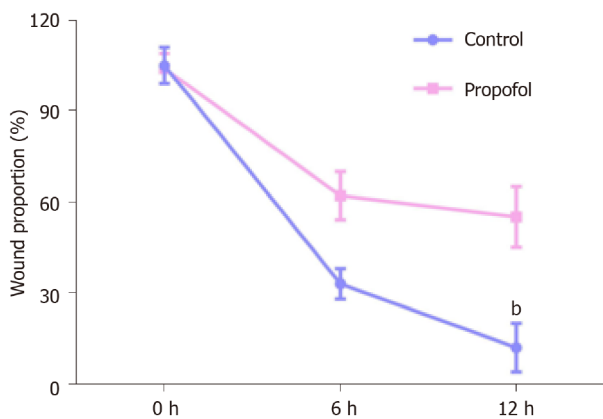
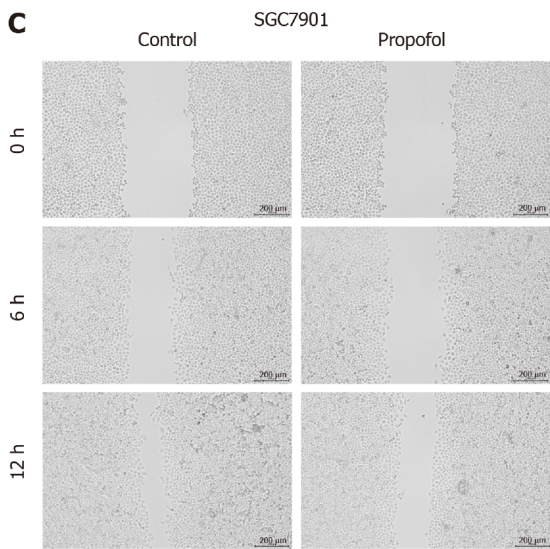
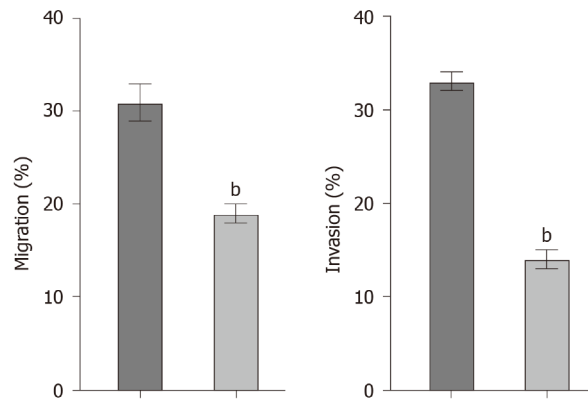
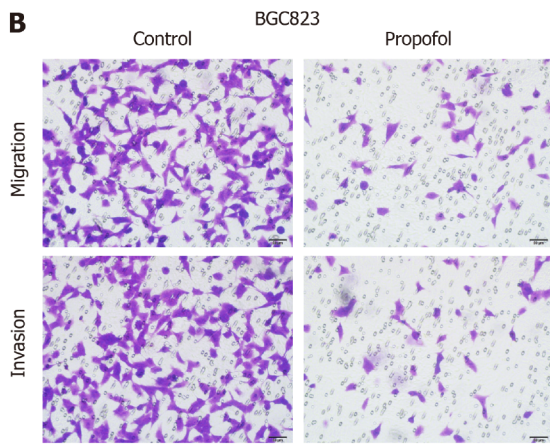
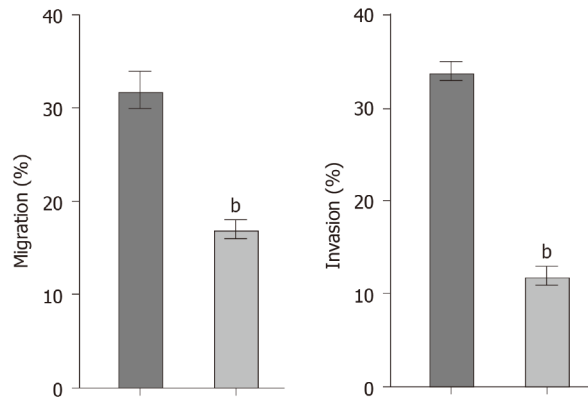
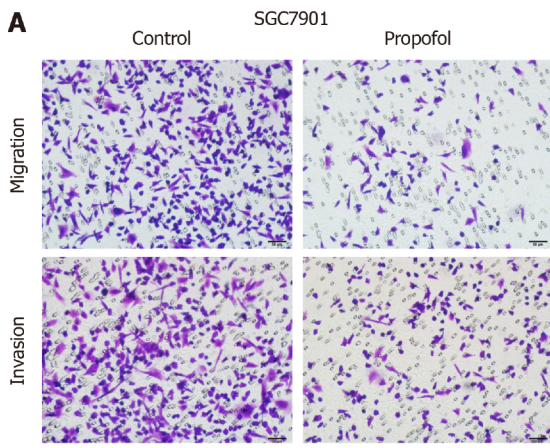


Figure 1 Propofol decreases proliferation and induces apoptosis of gastric cancer cells. A–E: SGC7901 and BGC823 cells were treated with propofol (10 μ mol/L). A and B: MTT assays analyzed cell viability; C and D: Colony formation assays measured cell proliferation; E and F: Flow cytometry analysis tested cell apoptosis. $n = 3$, mean \pm SD, ^b $P < 0.01$.



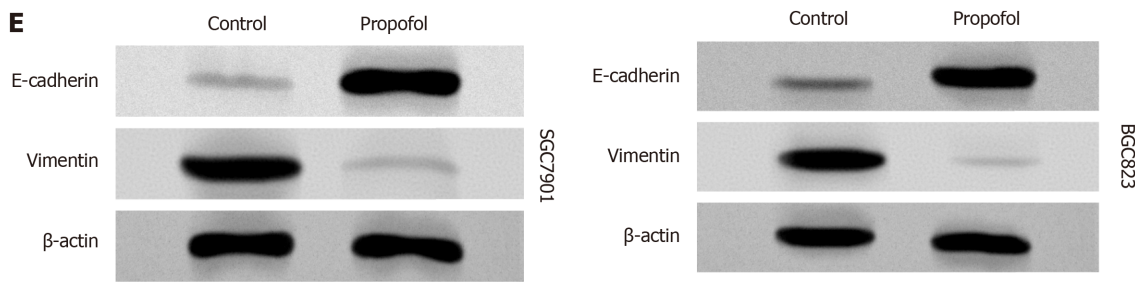


Figure 2 Propofol reduces invasion and migration of gastric cancer cells. A-D: SGC7901 and BGC823 cells were treated with propofol (10 $\mu\text{mol/L}$). A and B: Transwell assays analyzed cell migration and invasion; C and D: Wound healing assays examined migration and invasion. The wound healing proportion is shown. E: Protein levels of E-cadherin and vimentin were measured by western blotting. $n = 3$, mean \pm SD, $^bP < 0.01$.

125b-5p inhibitor promoted propofol-inhibited viability in SGC7901 and BGC823 cells (Figure 6A and B). Consistently, apoptosis of SGC7901 and BGC823 cells was induced by propofol, and overexpression of STAT3 or miR-125b-5p inhibitor reversed this effect in SGC7901 and BGC823 cells (Figure 6C), implying that propofol has an inhibitor effect on gastric cancer malignant phenotypes *via* the miR-125b-5p/STAT3 axis. We confirmed that propofol-induced levels of Fe^{2+} , iron and ROS were reversed by inhibition of miR-125b-5p in SGC7901 and BGC823 cells (Supplementary Figure 2).

Propofol attenuates growth of gastric cancer cells *in vivo*

We evaluated the effect of propofol on gastric cancer cell growth in a tumorigenicity analysis in nude mice. Tumor growth of SGC7901 or BGC823 cells was attenuated by propofol in nude mice (Figure 7A-C and Supplementary Figure 3A-C), as demonstrated by the reduced tumor size, weight and volume. As expected, expression of miR-125b-5p was enhanced and STAT3 expression was reduced in the tumor tissues of propofol-treated mice compared with the control group (Figure 7D and E and Supplementary Figure 3D and E). Expression of GPX4 and SLC7A11 was also down-regulated by propofol in the tumor tissues of mice (Figure 7F and Supplementary Figure 3F).

DISCUSSION

Gastric cancer is a prevalent malignancy with high mortality[1], in which ferroptosis plays a critical role in its development[6-8]. Propofol is a widely used anesthetic and has inhibitory effects on cancer progression. Nevertheless, the effect of propofol on ferroptosis during the development of gastric cancer is still unreported. In this study, we showed that propofol induced ferroptosis and inhibited malignant phenotypes of gastric cancer cells by regulating the miR-125b-5p/STAT3 axis.

Propofol has presented significant anticancer functions in several models. It has been reported that propofol inhibits the development of nonsmall cell lung cancer by downregulating the miR215p/MAPK10 axis[24]. Propofol represses malignant progression of pancreatic cancer cells by reducing NMDA receptor[25]. Propofol induces apoptosis of cervical cancer cells through inhibition of the HOTAIR/mTOR pathway[26]. Moreover, it has been found that propofol represses proliferation, migration and invasion by enhancing miR-195 in gastric cancer cells[14]. Propofol improves cisplatin sensitivity in gastric cancer by MALAT1/miR-30e/ATG5 signaling *via* inhibiting autophagy[27]. Propofol suppresses the survival and growth of gastric cancer by inducing expression of ING3[28]. We found that propofol decreased proliferation, migration and invasion and induced apoptosis of gastric cancer cells. Importantly, propofol enhanced ferroptosis in gastric cancer cells. Our data indicate an unreported function of propofol in the modulation of ferroptosis during gastric cancer progression, elucidating the novel role of the anesthetic in the ferroptosis of cancer development. Ferroptosis is one of the critical malignant phenotypes mediated by propofol in gastric cancer progression. The importance of ferroptosis and apoptosis should be compared by more complex investigations. Meanwhile, it has been reported that the regulation of ferroptosis may benefit the inhibition of gastric cancer development, and targeting ferroptosis may be a promising strategy for gastric cancer therapy.

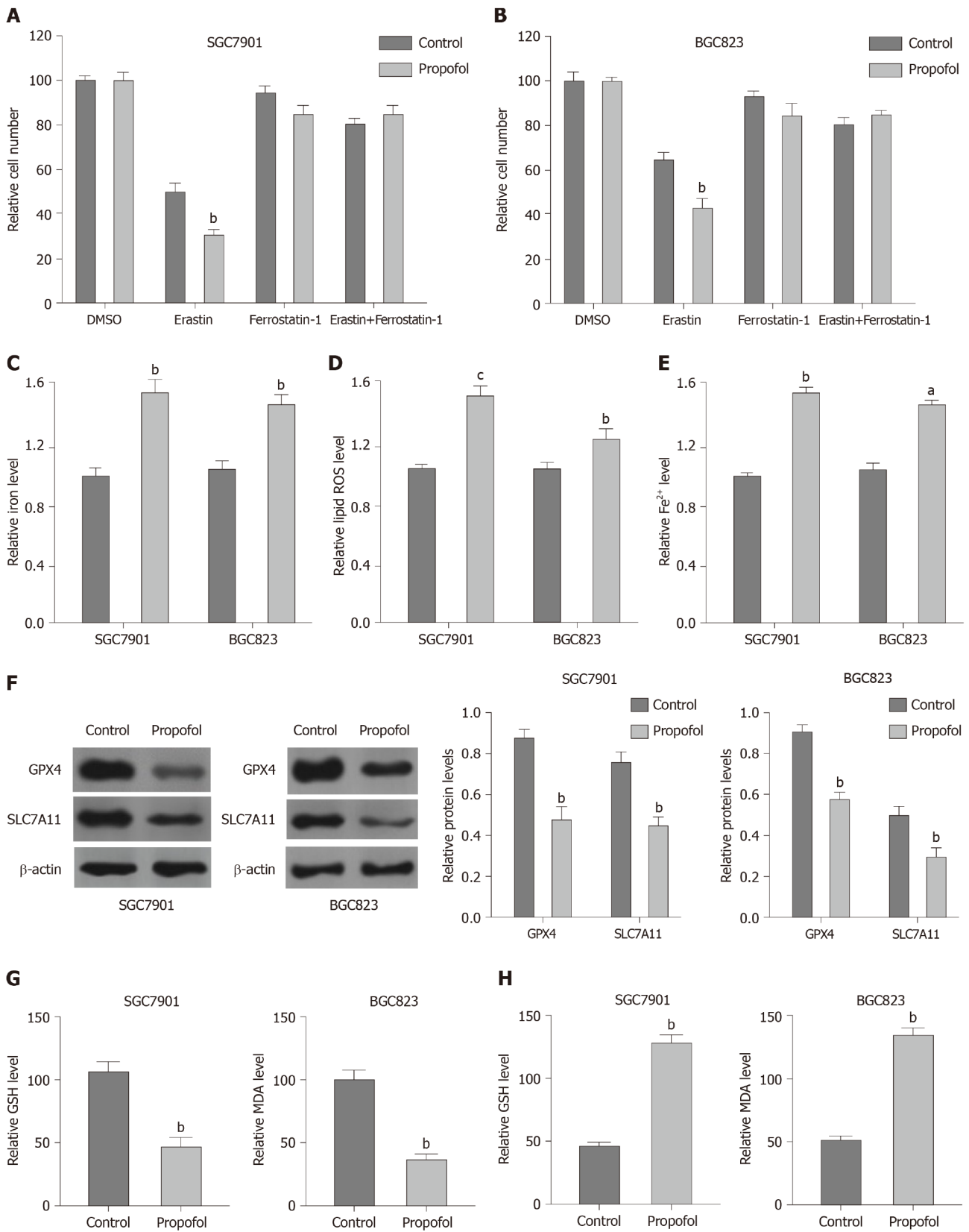


Figure 3 Propofol enhances ferroptosis in gastric cancer cells. A and B: SGC7901 and BGC823 were cotreated with 5 mmol/L erastin or ferrostatin (1 mmol/L) and propofol (10 μmol/L). Cell growth was analyzed by MTT assays. C–F: SGC7901 and BGC823 cells were treated with propofol (10 μmol/L). C: Flow cytometry measured the levels of ROS. D and E: Iron Assay Kit analyzed the levels of iron and Fe²⁺. F: Western blotting analysis tested the expression of GPX4, SLC7A11 and β-actin. G and H: Levels of GSH and MDA were analyzed by the detection kit. *n* = 3, mean ± SD, ^a*P* < 0.05, ^b*P* < 0.01, ^c*P* < 0.001.

miRNAs function as crucial regulators and are involved in gastric cancer progression. It has been reported that miR-96-5p enhances gastric cancer cell proliferation *via* inhibiting FOXO3[29]. miR-27b inhibits gastric cancer metastasis by

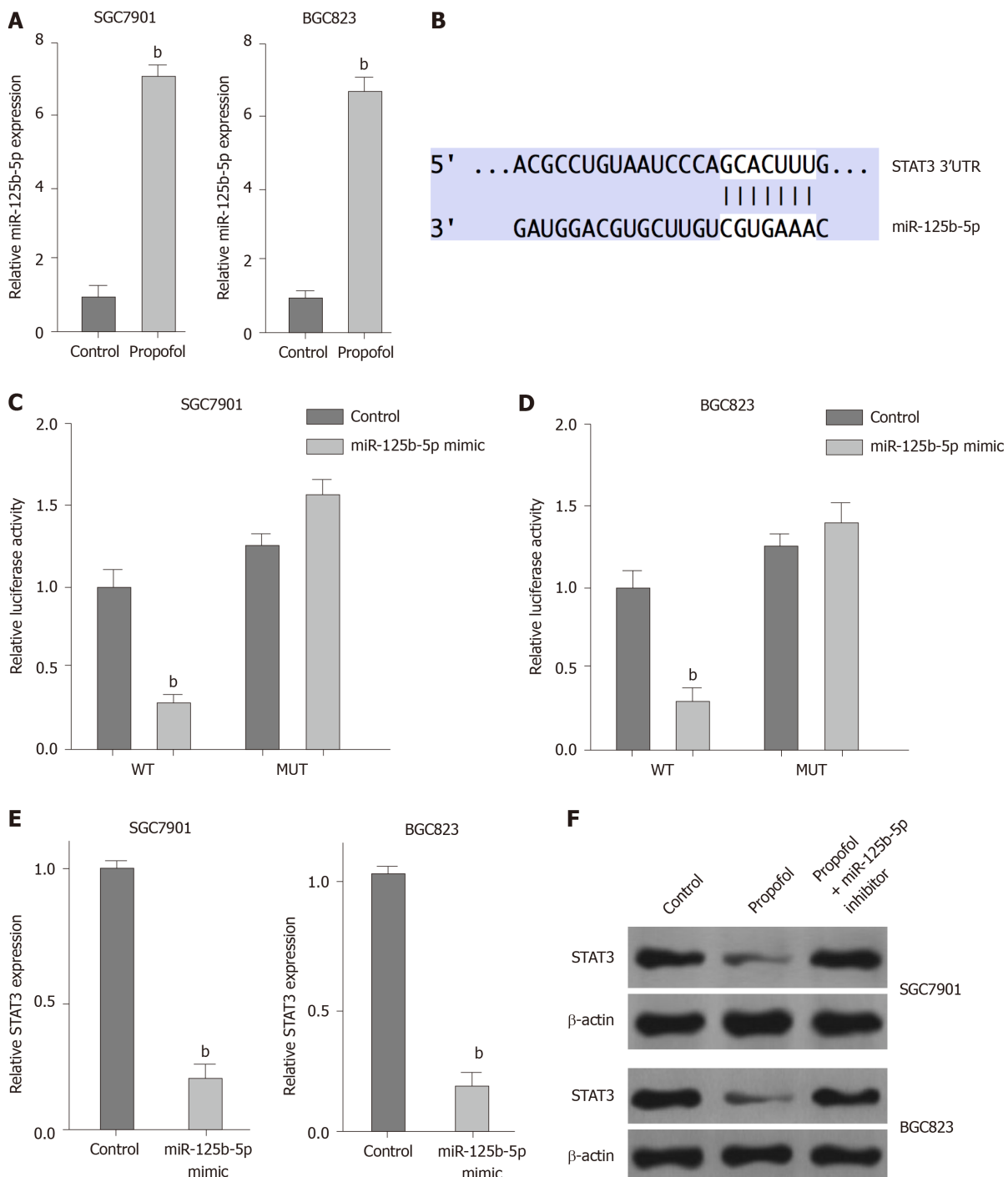


Figure 4 Propofol represses signal transducer and activator of transcription (STAT)3 expression by upregulating miR-125b-5p in gastric cancer cells. A: SGC7901 and BGC823 cells were treated with propofol (10 $\mu\text{mol/L}$). Quantitative reverse transcription polymerase chain reaction (qRT-PCR) measured expression of miR-125b-5p. B: The binding site of miR-125b-5p and STAT3 3' UTR was identified by bioinformatic analysis using Targetscan (http://www.targetscan.org/vert_72/). C–E: SGC7901 and BGC823 cells were treated with the miR-125b-5p mimic or control mimic. C and D: Luciferase reporter gene assays determined the luciferase activities. E: qRT-PCR analyzed mRNA expression of STAT3. F: SGC7901 and BGC823 cells were treated with propofol, or cotreated with propofol and miR-125b-5p inhibitor. Western blotting assessed protein expression of STAT3 and β -actin. $n = 3$, mean \pm SD, $^bP < 0.01$.

downregulating NR2F2 (nuclear receptor subfamily 2 group F member 2)[30]. miR-558 contributes to the progression of gastric cancer by repressing Smad4-regulated heparanase expression[31]. Moreover, it has been reported that miR-125b-5p represses invasion, migration and proliferation of breast cancer cells by inhibiting KIAA1522 [32]. miR-125b-5p suppresses invasion, migration and proliferation of hepatocellular carcinoma cell by downregulating thioredoxin reductase 1[33]. miR-125b-5p inhibits the progression of bladder cancer by attenuating PI3K/AKT signaling and targeting hexokinase 2[34]. In the present study, we found that propofol inhibited STAT3 expression by upregulating miR-125b-5p in gastric cancer cells. Propofol induced

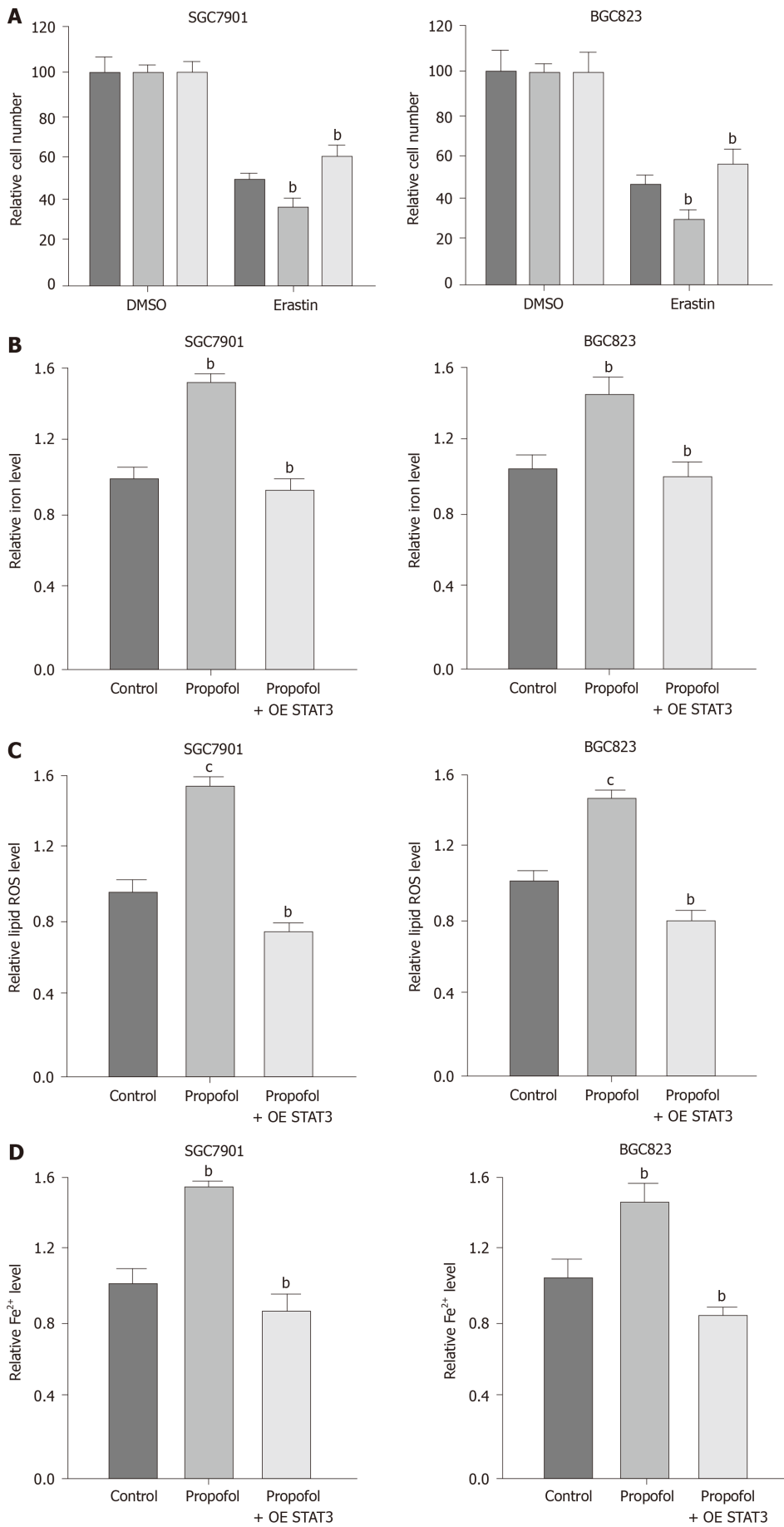


Figure 5 Propofol enhances ferroptosis by targeting signal transducer and activator of transcription (STAT)3 in gastric cancer cells. A:

SGC7901 and BGC823 cells were treated with 5 mmol/L erastin, cotreated with 5 mmol/L erastin and propofol, or cotreated with 5 mmol/L erastin, propofol, and pcDNA.1-STAT3. MTT assays measured cell growth. B–D: SGC7901 and BGC823 cells were treated with propofol, or cotreated with propofol and pcDNA.1-STAT3. B: Iron Assay Kit analyzed the levels of iron; C: Flow cytometry analysis tested the levels of ROS; and D: Iron Assay Kit analyzed the levels of Fe^{2+} . $n = 3$, mean \pm SD, ^b $P < 0.01$, ^c $P < 0.001$.

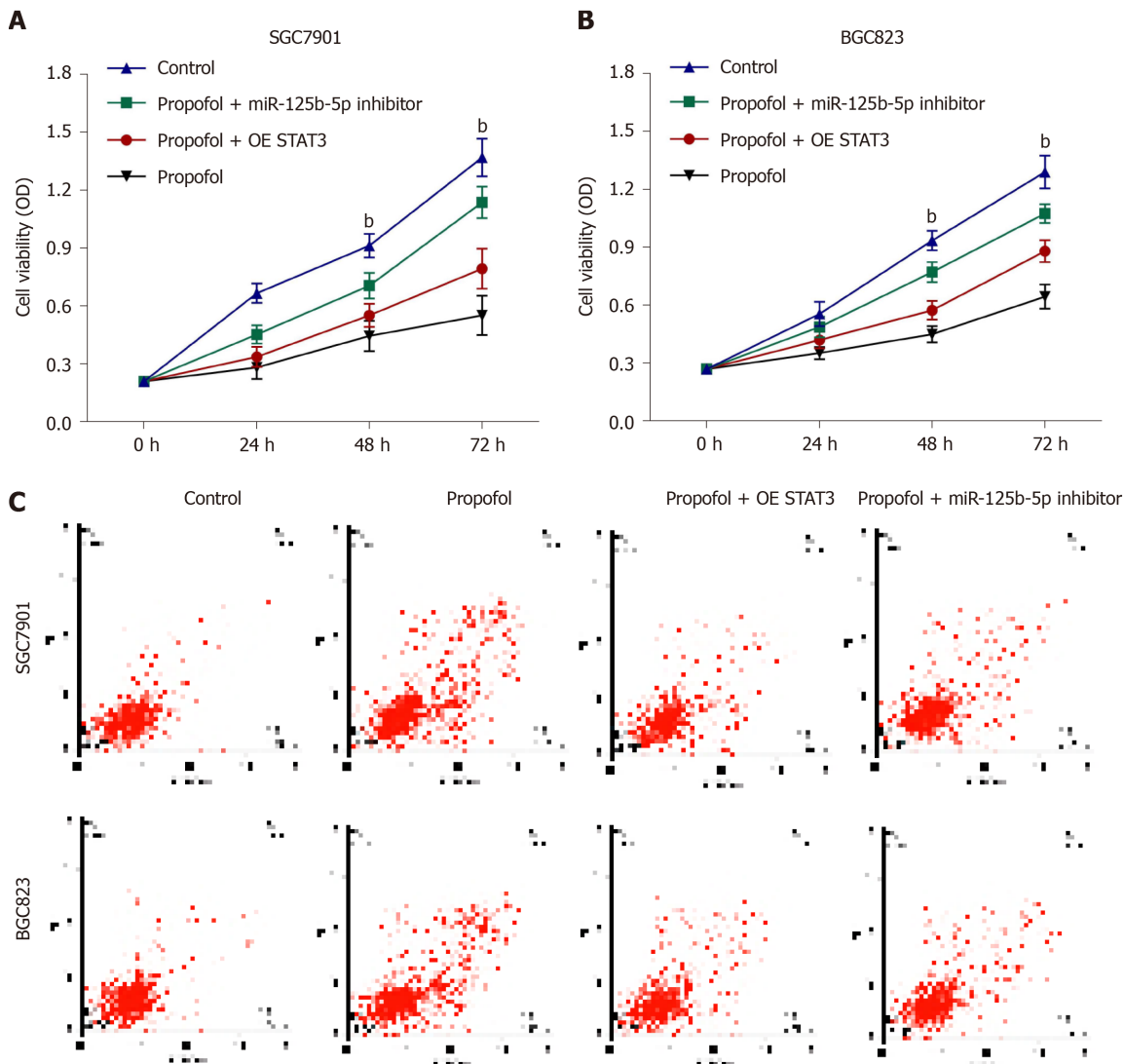


Figure 6 Propofol attenuates gastric cancer progression by miR-125b-5p/STAT3 axis. A–C: SGC7901 and BGC823 cells were treated propofol, or cotreated with propofol and miR-125b-5p inhibitor or pcDNA.1-STAT3. A and B: MTT assays analyzed the cell viability; C: Flow cytometry measured apoptosis. $n = 3$, mean \pm SD, ^b $P < 0.01$.

ferroptosis by targeting STAT3 in gastric cancer cells. The overexpression of STAT3 and miR-125b-5p inhibitor could reverse propofol-attenuated malignant phenotypes of gastric cancer cells. It uncovers a novel mechanism involving propofol, miR-125b-5p and STAT3 in the regulation of gastric cancer, enriching the understanding of the anticancer effect of propofol.

CONCLUSION

We discovered that propofol induced ferroptosis and inhibited malignant phenotypes of gastric cancer cells by regulating the miR-125b-5p/STAT3 axis. Propofol may serve as a potential therapeutic candidate for gastric cancer therapy.

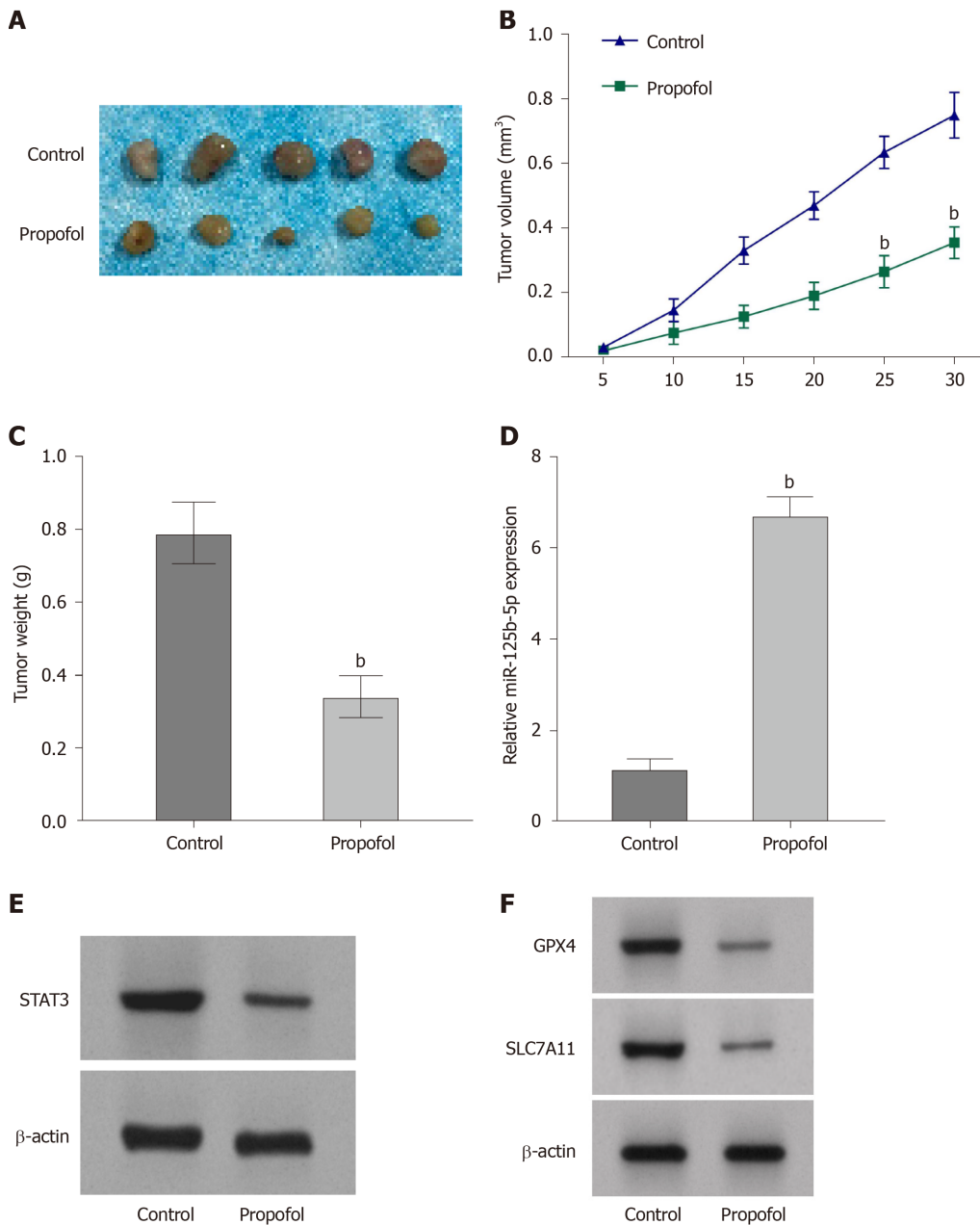


Figure 7 Propofol attenuates growth of gastric cancer cells *in vivo*. The nude mice were injected with SGC7901 cells and intraperitoneally treated with propofol (50 mg/kg). A: Tumor tissues; B: Tumor volume; and C: Tumor weight; D: Expression of miR-125b-5p was analyzed by quantitative reverse transcription polymerase chain reaction. E: Protein expression of STAT3 was detected by western blotting. F: Protein expression of GPX4 and SLC7A11 was measured by western blotting. *n* = 5, mean ± SD, ^b*P* < 0.01.

ARTICLE HIGHLIGHTS

Research background

Gastric cancer is a common malignancy with poor prognosis, in which ferroptosis plays a crucial role in its development. Propofol is a widely used anesthetic and has shown antitumor potential in gastric cancer. However, the effect of propofol on ferroptosis during gastric cancer progression remains unreported.

Research motivation

This study aims to identify the function of propofol in the regulation of ferroptosis and malignant phenotypes of gastric cancer cells.

Research objectives

To explore the role of propofol in the regulation of ferroptosis and malignant phenotypes of gastric cancer cells.

Research methods

MTT assays, colony formation assays, Transwell assays, wound healing assay, analysis of cell apoptosis, ferroptosis measurement, luciferase reporter gene assay and quantitative reverse transcription-PCR were used in this study.

Research results

Propofol was able to inhibit proliferation and induce apoptosis of gastric cancer cells. Propofol markedly repressed the invasion and migration of gastric cancer cells. Importantly, propofol enhanced the erastin-induced inhibitory effect on the growth of gastric cancer cells. Consistently, propofol increased the levels of ROS, iron and Fe²⁺ in gastric cancer cells. Propofol suppressed STAT3 expression by upregulating miR-125b-5p and propofol induced ferroptosis by targeting STAT3 in gastric cancer cells. The miR-125b-5p inhibitor or STAT3 overexpression could reverse propofol-attenuated malignant phenotypes of gastric cancer cells.

Research conclusions

Propofol induced ferroptosis and inhibited malignant phenotypes of gastric cancer cells by regulating the miR-125b-5p/STAT3 axis.

Research perspectives

Propofol may serve as a potential therapeutic candidate for gastric cancer therapy.

REFERENCES

- 1 **Smyth EC**, Nilsson M, Grabsch HI, van Grieken NC, Lordick F. Gastric cancer. *Lancet* 2020; **396**: 635-648 [PMID: 32861308 DOI: 10.1016/S0140-6736(20)31288-5]
- 2 **Machlowska J**, Baj J, Sitarz M, Maciejewski R, Sitarz R. Gastric Cancer: Epidemiology, Risk Factors, Classification, Genomic Characteristics and Treatment Strategies. *Int J Mol Sci* 2020; **21** [PMID: 32512697 DOI: 10.3390/ijms21114012]
- 3 **Sexton RE**, Al Hallak MN, Diab M, Azmi AS. Gastric cancer: a comprehensive review of current and future treatment strategies. *Cancer Metastasis Rev* 2020; **39**: 1179-1203 [PMID: 32894370 DOI: 10.1007/s10555-020-09925-3]
- 4 **Bekaii-Saab T**, El-Rayes B. Identifying and targeting cancer stem cells in the treatment of gastric cancer. *Cancer* 2017; **123**: 1303-1312 [PMID: 28117883 DOI: 10.1002/ncr.30538]
- 5 **Nehring H**, Meierjohann S, Friedmann Angeli JP. Emerging aspects in the regulation of ferroptosis. *Biochem Soc Trans* 2020; **48**: 2253-2259 [PMID: 33125483 DOI: 10.1042/BST20200523]
- 6 **Hao S**, Yu J, He W, Huang Q, Zhao Y, Liang B, Zhang S, Wen Z, Dong S, Rao J, Liao W, Shi M. Cysteine Dioxygenase 1 Mediates Erastin-Induced Ferroptosis in Human Gastric Cancer Cells. *Neoplasia* 2017; **19**: 1022-1032 [PMID: 29144989 DOI: 10.1016/j.neo.2017.10.005]
- 7 **Lee JY**, Nam M, Son HY, Hyun K, Jang SY, Kim JW, Kim MW, Jung Y, Jang E, Yoon SJ, Kim J, Seo J, Min JK, Oh KJ, Han BS, Kim WK, Bae KH, Song J, Huh YM, Hwang GS, Lee EW, Lee SC. Polyunsaturated fatty acid biosynthesis pathway determines ferroptosis sensitivity in gastric cancer. *Proc Natl Acad Sci U S A* 2020; **117**: 32433-32442 [PMID: 33288688 DOI: 10.1073/pnas.2006828117]
- 8 **Zhang H**, Deng T, Liu R, Ning T, Yang H, Liu D, Zhang Q, Lin D, Ge S, Bai M, Wang X, Zhang L, Li H, Yang Y, Ji Z, Wang H, Ying G, Ba Y. CAF secreted miR-522 suppresses ferroptosis and promotes acquired chemo-resistance in gastric cancer. *Mol Cancer* 2020; **19**: 43 [PMID: 32106859 DOI: 10.1186/s12943-020-01168-8]
- 9 **Vasileiou I**, Xanthos T, Koudouna E, Perrea D, Klonaris C, Katsargyris A, Papadimitriou L. Propofol: a review of its non-anaesthetic effects. *Eur J Pharmacol* 2009; **605**: 1-8 [PMID: 19248246 DOI: 10.1016/j.ejphar.2009.01.007]
- 10 **Liu Z**, Zhang J, Hong G, Quan J, Zhang L, Yu M. Propofol inhibits growth and invasion of pancreatic cancer cells through regulation of the miR-21/Slug signaling pathway. *Am J Transl Res* 2016; **8**: 4120-4133 [PMID: 27829997]
- 11 **Yang N**, Liang Y, Yang P, Yang T, Jiang L. Propofol inhibits lung cancer cell viability and induces cell apoptosis by upregulating microRNA-486 expression. *Braz J Med Biol Res* 2017; **50**: e5794 [PMID: 28076456 DOI: 10.1590/1414-431X20165794]
- 12 **Tsuchiya M**, Asada A, Arita K, Utsumi T, Yoshida T, Sato EF, Utsumi K, Inoue M. Induction and mechanism of apoptotic cell death by propofol in HL-60 cells. *Acta Anaesthesiol Scand* 2002; **46**: 1068-1074 [PMID: 12366500 DOI: 10.1034/j.1399-6576.2002.460903.x]
- 13 **Ai L**, Wang H. Effects of propofol and sevoflurane on tumor killing activity of peripheral blood natural killer cells in patients with gastric cancer. *J Int Med Res* 2020; **48**: 300060520904861 [PMID: 32216484 DOI: 10.1177/0300060520904861]
- 14 **Zhang W**, Wang Y, Zhu Z, Zheng Y, Song B. Propofol inhibits proliferation, migration and invasion of gastric cancer cells by up-regulating microRNA-195. *Int J Biol Macromol* 2018; **120**: 975-984

- [PMID: 30171944 DOI: 10.1016/j.ijbiomac.2018.08.173]
- 15 **Sayed D**, Abdellatif M. MicroRNAs in development and disease. *Physiol Rev* 2011; **91**: 827-887 [PMID: 21742789 DOI: 10.1152/physrev.00006.2010]
 - 16 **Huangfu L**, He Q, Han J, Shi J, Li X, Cheng X, Guo T, Du H, Zhang W, Gao X, Luan F, Xing X, Ji J. MicroRNA-135b/CAMK2D Axis Contribute to Malignant Progression of Gastric Cancer through EMT Process Remodeling. *Int J Biol Sci* 2021; **17**: 1940-1952 [PMID: 34131397 DOI: 10.7150/ijbs.58062]
 - 17 **Miliotis C**, Slack FJ. miR-105-5p regulates PD-L1 expression and tumor immunogenicity in gastric cancer. *Cancer Lett* 2021; **518**: 115-126 [PMID: 34098061 DOI: 10.1016/j.canlet.2021.05.037]
 - 18 **Deng P**, Sun M, Zhao WY, Hou B, Li K, Zhang T, Gu F. Circular RNA circVAPA promotes chemotherapy drug resistance in gastric cancer progression by regulating miR-125b-5p/STAT3 axis. *World J Gastroenterol* 2021; **27**: 487-500 [PMID: 33642823 DOI: 10.3748/wjg.v27.i6.487]
 - 19 **Ashrafizadeh M**, Zarrabi A, Orouei S, Zarrin V, Rahmani Moghadam E, Zabolian A, Mohammadi S, Hushmandi K, Gharehaghajlou Y, Makvandi P, Najafi M, Mohammadinejad R. STAT3 Pathway in Gastric Cancer: Signaling, Therapeutic Targeting and Future Prospects. *Biology (Basel)* 2020; **9** [PMID: 32545648 DOI: 10.3390/biology9060126]
 - 20 **Cafferkey C**, Chau I. Novel STAT 3 inhibitors for treating gastric cancer. *Expert Opin Investig Drugs* 2016; **25**: 1023-1031 [PMID: 27322026 DOI: 10.1080/13543784.2016.1195807]
 - 21 **Pan YM**, Wang CG, Zhu M, Xing R, Cui JT, Li WM, Yu DD, Wang SB, Zhu W, Ye YJ, Wu Y, Wang S, Lu YY. STAT3 signaling drives EZH2 transcriptional activation and mediates poor prognosis in gastric cancer. *Mol Cancer* 2016; **15**: 79 [PMID: 27938379 DOI: 10.1186/s12943-016-0561-z]
 - 22 **Gao Y**, Yu X, Zhang F, Dai J. Propofol inhibits pancreatic cancer progress under hypoxia via ADAM8. *J Hepatobiliary Pancreat Sci* 2019; **26**: 219-226 [PMID: 30945470 DOI: 10.1002/jhbp.624]
 - 23 **Zhang YF**, Li CS, Zhou Y, Lu XH. Effects of propofol on colon cancer metastasis through STAT3/HOTAIR axis by activating WIF-1 and suppressing Wnt pathway. *Cancer Med* 2020; **9**: 1842-1854 [PMID: 31953926 DOI: 10.1002/cam4.2840]
 - 24 **Wu X**, Li X, Xu G. Propofol suppresses the progression of nonsmall cell lung cancer via downregulation of the miR215p/MAPK10 axis. *Oncol Rep* 2020; **44**: 487-498 [PMID: 32468043 DOI: 10.3892/or.2020.7619]
 - 25 **Chen X**, Wu Q, You L, Chen S, Zhu M, Miao C. Propofol attenuates pancreatic cancer malignant potential via inhibition of NMDA receptor. *Eur J Pharmacol* 2017; **795**: 150-159 [PMID: 27986626 DOI: 10.1016/j.ejphar.2016.12.017]
 - 26 **Zhang D**, Zhou XH, Zhang J, Zhou YX, Ying J, Wu GQ, Qian JH. Propofol promotes cell apoptosis via inhibiting HOTAIR mediated mTOR pathway in cervical cancer. *Biochem Biophys Res Commun* 2015; **468**: 561-567 [PMID: 26523512 DOI: 10.1016/j.bbrc.2015.10.129]
 - 27 **Zhang YF**, Li CS, Zhou Y, Lu XH. Propofol facilitates cisplatin sensitivity via lncRNA MALAT1/miR-30e/ATG5 axis through suppressing autophagy in gastric cancer. *Life Sci* 2020; **244**: 117280 [PMID: 31926239 DOI: 10.1016/j.lfs.2020.117280]
 - 28 **Yang C**, Gao J, Yan N, Wu B, Ren Y, Li H, Liang J. Propofol inhibits the growth and survival of gastric cancer cells *in vitro* through the upregulation of ING3. *Oncol Rep* 2017; **37**: 587-593 [PMID: 27840947 DOI: 10.3892/or.2016.5218]
 - 29 **He X**, Zou K. MiRNA-96-5p contributed to the proliferation of gastric cancer cells by targeting FOXO3. *J Biochem* 2020; **167**: 101-108 [PMID: 31598681 DOI: 10.1093/jb/mvz080]
 - 30 **Feng Q**, Wu X, Li F, Ning B, Lu X, Zhang Y, Pan Y, Guan W. miR-27b inhibits gastric cancer metastasis by targeting NR2F2. *Protein Cell* 2017; **8**: 114-122 [PMID: 27844448 DOI: 10.1007/s13238-016-0340-z]
 - 31 **Zheng L**, Jiao W, Song H, Qu H, Li D, Mei H, Chen Y, Yang F, Li H, Huang K, Tong Q. miRNA-558 promotes gastric cancer progression through attenuating Smad4-mediated repression of heparanase expression. *Cell Death Dis* 2016; **7**: e2382 [PMID: 27685626 DOI: 10.1038/cddis.2016.293]
 - 32 **Li Y**, Wang Y, Fan H, Zhang Z, Li N. miR-125b-5p inhibits breast cancer cell proliferation, migration and invasion by targeting KIAA1522. *Biochem Biophys Res Commun* 2018; **504**: 277-282 [PMID: 30177391 DOI: 10.1016/j.bbrc.2018.08.172]
 - 33 **Hua S**, Quan Y, Zhan M, Liao H, Li Y, Lu L. miR-125b-5p inhibits cell proliferation, migration, and invasion in hepatocellular carcinoma via targeting TXNRD1. *Cancer Cell Int* 2019; **19**: 203 [PMID: 31384178 DOI: 10.1186/s12935-019-0919-6]
 - 34 **Liu S**, Chen Q, Wang Y. MiR-125b-5p suppresses the bladder cancer progression via targeting HK2 and suppressing PI3K/AKT pathway. *Hum Cell* 2020; **33**: 185-194 [PMID: 31605287 DOI: 10.1007/s13577-019-00285-x]



Published by **Baishideng Publishing Group Inc**
7041 Koll Center Parkway, Suite 160, Pleasanton, CA 94566, USA
Telephone: +1-925-3991568
E-mail: bpgoffice@wjgnet.com
Help Desk: <https://www.f6publishing.com/helpdesk>
<https://www.wjgnet.com>

